Optical characteristics of sapphire laser scalpels analysed by ray-tracing

Verdaasdonck, Rudolf, Borst, Cornelius

Rudolf M. Verdaasdonck, Cornelius Borst M.D., "Optical characteristics of sapphire laser scalpels analysed by ray-tracing," Proc. SPIE 1420, Optical Fibers in Medicine VI, (1 July 1991); doi: 10.1117/12.43874

SPIE.

Event: Optics, Electro-Optics, and Laser Applications in Science and Engineering, 1991, Los Angeles, CA, United States

OPTICAL CHARACTERISTICS OF SAPPHIRE LASER SCALPELS ANALYSED BY RAY-TRACING

Rudolf M. Verdaasdonk and Cornelius Borst

Department of Cardiology and Department of Medical Instrumentation, University Hospital Utrecht and the Interuniversity Cardiology Institute of the Netherlands, Utrecht, The Netherlands

ABSTRACT

For laser surgery, high power densities of light may be obtained by guiding a beam through the tapered end of a fiber or through a tapered rod. Due to the decreasing cross-sectional area of the taper, the power density increases until the beam refracts out of the taper. Ray-tracing was used to determine the irradiance distribution and power density within and at the tip of laser scalpels made of sapphire in relation to their geometry in air and in water. Computed beam profiles were compared to photographed profiles. The beams were emitted in cones with discrete angles which were related to the number of reflections within the scalpel. For taper angles as small as 5 degrees, the increase in power density exceeded 500x. Assuming the scalpel tip to be hemispherical rather than pointed or flat, the increase was 10-30 % smaller due to internal reflection losses. The design of laser scalpels may be adapted to obtain adequate power density for effective tissue cutting together with radial energy leaking to promote coagulation and hemostasis.

1. INTRODUCTION

Biological tissues may be cut with lasers to reduce mechanical trauma and/or to reduce bleeding[1]. The CO_2 laser light (10.6 μm) which is highly absorbed by tissue, cuts efficiently but the hemostatic effect is minimal. The hemostatic effect of lasers emitting light with wavelengths that are less absorbed by tissue is higher. However, for tissue cutting a suffiently high irradiance[2] needs to be realised.

High fluence rates of laser light may be obtained by focusing the beam by means of a lens or by guiding the beam through the tapered end of a fiber [3] or a tapered rod [4-6]. As the cross-sectional area of the rod decreases, the fluence rate increases until the beam starts to refract out of the taper usually with a large divergence angle. In contact with tissue, the high power density of the light at the point of the tapered end initiates tissue ablation[4]. Because of the large divergence angle of the exit beam, the irradiance decreases rapidly distal from the tip minimizing injury to adjacent tissue [5].

The optical behavior of the laser scalpels depends on the geometry of the scalpel, the beam diameter and beam divergence of the fiber, the refractive index of the scalpel and the refractive index of the medium. By means of ray-tracing, the optical behavior of laser scalpels was analysed in relation to these parameters to determine the irradiance distribution and increase in fluence rate within and at the tip of the scalpel. The computed beam profiles were compared with photographed beam profiles. This paper is part of a more detailed study published elsewhere [7].

2. METHODS

2.1 Ray-tracing program

A ray-tracing program was developed in Quickbasic (Microsoft) for the calculation of the beam profile and irradiance distribution inside and outside the scalpels. The program traced 850 rays equally divided along a line at the entrance of the scalpel covering a 10 degree divergence angle. At every transition which an individual ray encountered, either the total reflectance angle or the refraction angle was calculated according to Fresnels laws of reflection and refraction [8]. In case of refraction, the intensity loss due to reflection at the transition was

0-8194-0510-8/91/$4.00

neglected because for angles of incidence up to 5 degrees near the critical angle, the loss is below 10 % in air and below 3 % in water.

2.2 Scalpel configuration

The geometry of the tapered laser scalpels was defined by the taper angle α (Fig.1A). The scalpels were assumed to be made of sapphire having a refractive index of 1.75. The taper angle was varied from 1 to 45 degrees. A ray reflected several times up and down the scalpel before its angle with respect to the scalpel surface exceeded the angle of total reflection. Then the ray refracted ('leaked') out of the scalpel (Fig.1A). The scalpel was assumed to end in a point, in a flat tip with a diameter $2R_p$ or in a hemispherical tip with a radius R_p (Fig.1).

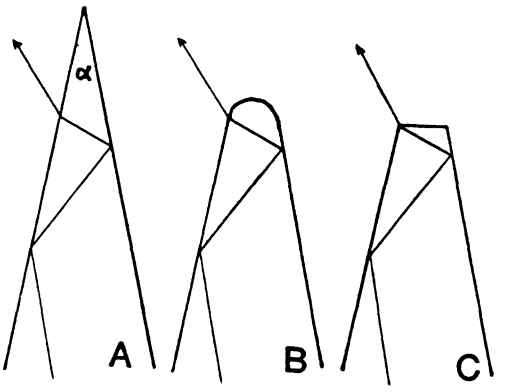

Figure 1: (A) A ray will be reflected up and down inside a tapered rod with angle α until the angle of incidence relative to the surface exceeds the critical angle and the ray is refracted out of the scalpel. The point of the tapered rod may end in either a hemispherical (B) or a flat tip (C).

2.3 Calculations

The program produced a graphic representation of the beam profile. The position was determined where the rays started to refract ('leak') out of the scalpel in relation to the taper angle. The irradiance distribution and the total energy were calculated at 20 equally spaced cross-sections along twice the length of the 'leaking' part of the scalpel. The irradiance distributions were combined to an iso-irradiance level map within the scalpel point. The increase in power density inside the scalpel and at the tip was calculated in air and in water, normalized to the power density at the entrance of the scalpel.

2.4 Measurements

Scalpels were analysed with taper angles of 4 and 16 degrees ending in a flat and hemispherical tip, respectively. The beam profiles of the probes were photographed in water with scattering ink particles.

3. RESULTS

3.1 Beam profiles

The calculated and photographed beam profiles in water of the 16 and 4 degree scalpels are presented in the compositions of Figures 2 and 3, respectively.

3.2 'Leaking' length of the scalpel

The calculated length of the scalpel at the level where the first rays refracted out of the scalpel in relation to the taper angle is shown in Figure 4. The 'leaking' length changed in large discrete steps. In air, the rays reflected further down into the scalpel tip than in water.

3.3 Irradiance distribution

The iso-irradiance maps for taper angles of 16 and 4 degrees are included in the compositions of Figures 2 and 3, respectively.

3.4 Power density increase

The power density increase towards the scalpel tip is presented in Figure 5 for taper angles of 5, 15 and 30 degrees. The distance to the tip was normalized to the 'leaking' length of the scalpel. The increase was calculated relative to the magnitude at the entrance of the scalpel. For taper angles as small as 5 degrees, the increase at the level the scalpel started 'leaking' was 50x in air and 30x in water and exceeded 500x further towards the tip. Assuming the scalpel tip to be hemispherical rather than flat (Fig.1), the power density increase was 10-30 % smaller due to internal reflection losses.

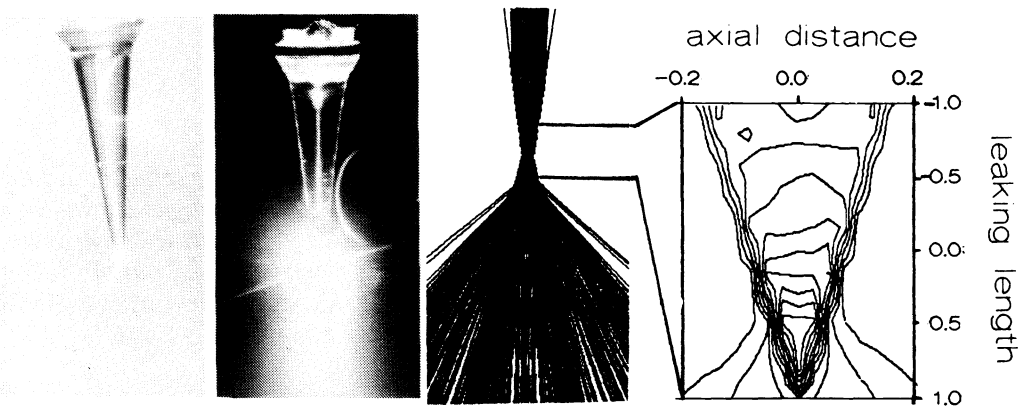

Figure 2: From left to right panel: photo scalpel, calculated beam, photographed beam and irradiance distribution of the 16 degree tapered scalpel (MTRP 5.0, Surgical Laser Technologies, Malvern, PA, USA) in water.

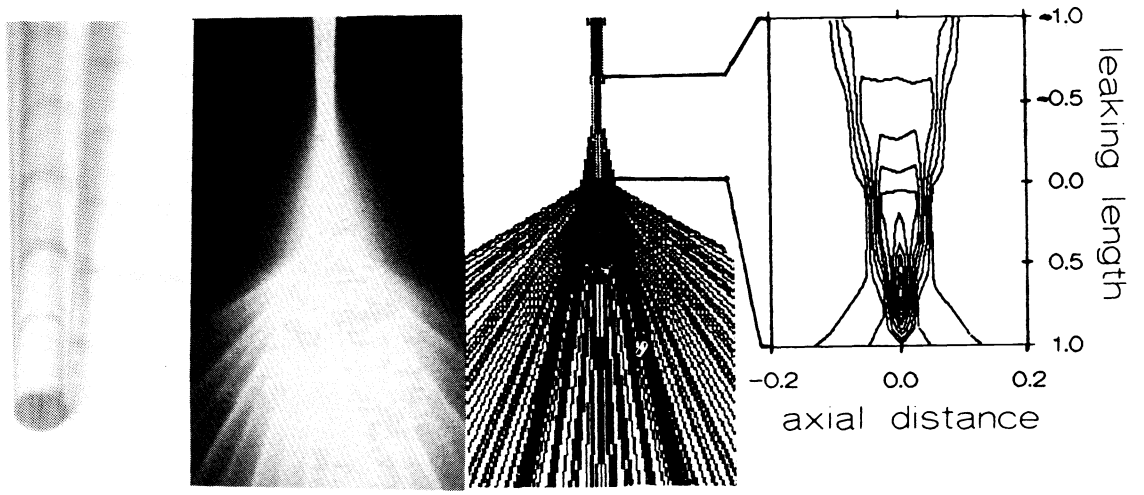

Figure 3: From left to right panel: photo scalpel, calculated beam, photographed beam and irradiance distribution of the 4 degree tapered scalpel with a flat tip in water.

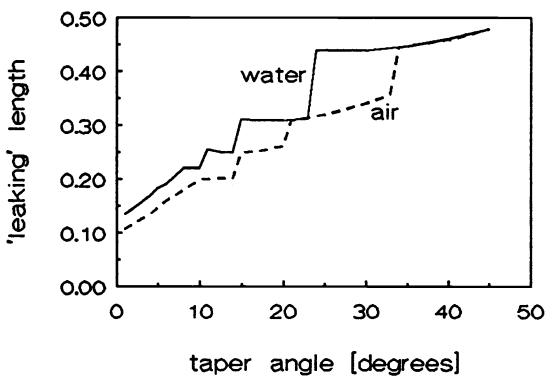

Figure 4: 'Leaking' length along the scalpel where rays refract out of the scalpel in relation to the taper angle in air (dotted curve) and water (solid curve). The 'leaking' length was normalized with respect to the total length of the scalpel relative to the tip.

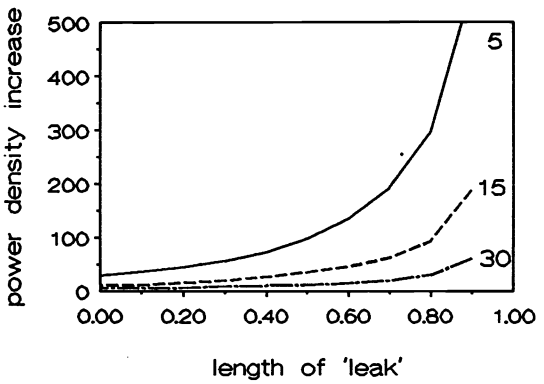

Figure 5: increase in power density relative to the power density at the entrance of the scalpel for 5, 15, and 30 degrees taper angles. The 'leaking' length was normalized with respect to the total length of the scalpel relative to the tip.

4. DISCUSSION

4.1 Beam profiles

The computed profiles showed the presence of one dominant, conically shaped beam emerging from the pointed tip (Fig.2). When the scalpel ended in a flat point the profile consisted of several conically shaped beams at discrete angles (Fig.3). These angles were related to the number of reflections inside the scalpel before the ray refracted out of the scalpel. The angle of each cone depended on the starting position of a ray relative to the optical axis and on its starting angle. The discrete angles were no longer present when the tip ended in a hemispherical tip.

On the photographs, it was sometimes difficult to distinguish the complete beam profile. Due to the high irradiance at the tip, the diverging beam was outshined. The best results were obtained in water due to index matching (Figs.2 and 3). As far as could be distinguished, the calculated and photographed profiles were similar.

4.2 'Leaking' length of the scalpel

Depending on the taper angle, the normalized length of the scalpel where rays started to leak out, changed in discrete steps (Fig.4). These steps were related to the number of reflections inside the scalpel. A small decrease in the taper angle could result in an additional internal reflection of a ray. The ray would then refract out of the scalpel on the opposite side further towards the tip.

4.3 Irradiance distribution

The iso-irradiance maps (Figs.2 and 3) showed that the position and the dimensions of the area of highest irradiance depended on the taper angle. For large taper angles, the irradiance did not increase dramatically once the scalpel started leaking. For small taper angles, in contrast, the highest irradiance was concentrated in the very tip. Due to limited spatial resolution of the ray-tracing, the iso-irradiance maps are not totally symmetrical.

4.4 Irradiance increase

Once rays started to refract out of the scalpel, the total power decreased towards the tip. The power density increase towards the tip due to the the decrease of the cross-sectional surface area, outnumbered the decrease of the total power inside the scalpel. For smaller taper angles a power density increase over 500 times relative to the power density at the entrance of the scalpel was achieved (Fig.5). In practice, this increase is limited by the mechanical strength of the point which will break when is becomes too small.

4.5 Probe design for cutting and coagulating

The laser may be used as an alternative to the surgical knife. One major advantage is the capability to combine cutting with tissue coagulation. Using a wavelength with a high tissue penetration depth like Nd:YAG [9,10], small blood vessels in highly perfused organs will be coagulated during cutting. In this way surgical procedures like liver resections [11] may be performed with minimal loss of blood.

The irradiance at the scalpel point may be controlled by shortening the tip of the scalpels to the level of the desired irradiance increase to cut effectively in combination with a sufficient 'leaking' length for adequate hemostasis. If the point is cut flat, the point has sharp edges like a bare fiber. Spherically tipped scalpels, on the other hand, appeared to have in water internal reflection losses of 10 to 20 percent .

5. CONCLUSIONS

Laser scalpels emitted the laser beam in a cone shape. The angle of this cone was related to the number of reflections inside the scalpel. Within the scalpel, the power density may increase several hunderd times.

The scalpel tip may be shortened to obtain a sufficient power density for effective tissue cutting combined with radial energy leaking to promote coagulation and hemostatic effects.

6. ACKNOWLEDGEMENTS

RMV was supported by The Netherlands Heart Foundation (grant 87.073).

7. REFERENCES

1. Wiemann TJ. Lasers and the surgeon. Am J Surg 1986; 151:493-500.
2. Welch AJ. Laser irradiation of tissue. In 'Heat transfer in medicine and biology' Vol.2. Shitzer A, Eberhart RC (eds.), Plenum Press, New York, 1985: 135-184.
3. Chang CT, Auth DC. Radiation characteristics of a tapered cylindrical optical fiber. J Opt Soc Am 1978; 68:1191-1196.
4. Hukki J, Krogerus L, Castren M, Schroder T. Effects of different contact laser scalpels on skin and subcutaneous fat. Lasers Surg Med 1988; 8:276-282.
5. Kim LY Jr, Day AL, Normann SJ, Abela GS, Mehta JL. The argon contact laser scalpel: a study of its effect on atherosclerosis. Neurosurgery 1987; 21:861-866.
6. Kim LY Jr, Roxey TE, Day AL. The argon "contact" laser scalpel: technical considerations. Neurosurgery 1987; 21:858-860.
7. Verdaasdonk RM, Borst C. Ray-tracing of optically modified fiber tips II: Laser scalpels. Applied Optics 1991 (conditionally accepted).
8. Hecht E, Zajac A. Optics. Reading, Mass.: Addison-Wesley 1979:60-98.
9. Rosenfeld H, Sherman R. Treatment of cutaneous and deep vascular lesions with the Nd:YAG laser. Lasers Surg Med 1986; 6:20-3.
10. Daikuzono N, Joffe SN. Artificial sapphire probe for contact photocoagulation and tissue vaporization with the Nd:YAG laser. Med Instrum 1985; 192:173-178.
11. Joffe SN. Resection of the liver with the Nd:YAG laser. Surg Gyn Obstet 1986; 163:437-442.